

# AMIGO2 characterizes cancer-associated fibroblasts in metastatic colon cancer and induces the release of paracrine active tumorigenic secretomes

Yongsong Yong<sup>1,2</sup>, Richard Demmler<sup>1</sup>, Bisan Abdalfatah Zohud<sup>1</sup>, Qi Fang<sup>1</sup>, Tong Zhang<sup>2</sup>, Yonghua Zhou<sup>2</sup>, Katja Petter<sup>1</sup>, Christian Flierl<sup>1</sup>, Tobias Gass<sup>1</sup>, Carol I Geppert<sup>3</sup>, Susanne Merkel<sup>4</sup>, Vera S Schellerer<sup>4,5</sup>, Elisabeth Naschberger<sup>1,6,7,8†</sup> and Michael Stürzl<sup>1,6,7,8\*†</sup>

<sup>1</sup> Division of Molecular and Experimental Surgery, Department of Surgery, Universitätsklinikum Erlangen, Friedrich-Alexander-Universität (FAU) Erlangen-Nürnberg, Erlangen, Germany

<sup>2</sup> Xinghua People's Hospital Affiliated to Yangzhou University, Taizhou, PR China

<sup>3</sup> Institute of Pathology, Universitätsklinikum Erlangen, Friedrich-Alexander-Universität (FAU) Erlangen-Nürnberg, Erlangen, Germany

<sup>4</sup> Department of Surgery, Universitätsklinikum Erlangen, Friedrich-Alexander-Universität (FAU) Erlangen-Nürnberg, Erlangen, Germany

<sup>5</sup> Department of Pediatric Surgery, University Medicine Greifswald, Greifswald, Germany

<sup>6</sup> CCC Erlangen-EMN: Comprehensive Cancer Center Erlangen-EMN (CCC ER-EMN), Universitätsklinikum Erlangen, Friedrich-Alexander-Universität (FAU) Erlangen-Nürnberg, Erlangen, Germany

<sup>7</sup> CCC WERA: Comprehensive Cancer Center Alliance WERA (CCC WERA), Erlangen, Germany

<sup>8</sup> BZKF: Bavarian Cancer Research Center (BZKF), Erlangen, Germany

\*Correspondence to: M Stürzl, Division of Molecular and Experimental Surgery, Translational Research Center (TRC), Universitätsklinikum Erlangen, Kussmaulallee 12, D-91054 Erlangen, Germany. E-mail: michael.stuerzl@uk-erlangen.de

†These authors contributed equally to this work.

## Abstract

Secretomes of cancer-associated fibroblasts (CAFs) in colorectal cancer (CRC) contribute to malignancy. Detailed knowledge is available on the components and functions of CAF secretomes. Little is known about the regulation of CAF secretomes. Here, we searched for receptor-like membrane-bound molecules in CAFs, which may regulate the production and release of tumor-activating secretomes. The adhesion molecule with Ig-like domain 2 (AMIGO2) was significantly upregulated in cultivated CAFs compared to normal tissue-associated fibroblasts (NAFs), and this was confirmed in patient-derived tissues. AMIGO2 expression was low or absent in healthy colon, significantly increased in fibroblasts of primary CRC, and highest in the stromal tissues of CRC-derived liver metastases. AMIGO2 expression in CAFs correlated with a higher T-category, increased lymph node metastasis, progressed tumor stages and was associated with reduced survival in different cohorts of CRC patients. Interestingly, AMIGO2 expression was induced by transforming growth factor- $\beta$  and higher in female patients, who exhibit a more aggressive disease course. In functional studies, conditioned media of NAFs with experimentally induced AMIGO2 overexpression enhanced proliferation and migration of different CRC tumor cells, while siRNA-mediated inhibition of AMIGO2 in CAFs attenuated these effects. Accordingly, therapeutic inhibition of the receptor-like AMIGO2 protein in CRC CAFs could prevent tumorigenic secretomes in CRC.

© 2024 The Author(s). *The Journal of Pathology* published by John Wiley & Sons Ltd on behalf of The Pathological Society of Great Britain and Ireland.

**Keywords:** colorectal cancer; cancer-associated fibroblasts; tumor microenvironment; secretomes; secretion

Received 25 March 2024; Revised 24 July 2024; Accepted 1 October 2024

No conflicts of interest were declared.

## Introduction

The tumor microenvironment (TME) is established within a complex local interaction network of the tumor cells with different stromal cells, including immune cells, endothelial cells, and fibroblasts [1]. Meanwhile, it is well established and generally accepted that the TME plays a key role in cancer progression, therapy

response, and relapse. Intercellular communication in the TME is predominantly mediated by soluble proteins, which are released from one cell and bind to specific receptors on the surface of neighboring cells, thereby eliciting corresponding responses. A detailed characterization of colorectal cancer (CRC) whole-tumor transcriptomes identified mesenchymal gene signatures that are associated with poor prognosis of patients, further underscoring the impact of the TME and

particularly of cancer-associated fibroblasts (CAFs) in the progression of solid tumors such as CRC [2].

CAFs are among the best-studied stromal components within the TME of CRC, because these cells constitute nearly 70% of the cells in tumor tissues and are relatively easy to cultivate from normal and diseased tissues [3–5]. The characterization of CRC-derived CAFs revealed that these cells are highly plastic and present as different subtypes in tumor tissues, including inflammatory and myofibroblast-like CAFs [6]. CAFs interact reciprocally with the tumor cells through the release of complex secretomes composed of different cytokines, growth factors, matrix proteinases, and extracellular matrix (ECM) components [7–10]. Through these components, CAF secretomes regulate the phenotype of cancer cells, including migration, invasion, and proliferation, and trigger the remodeling of the normal ECM to a cancer-associated ECM.

In contrast to the detailed insight into the functions of CAF secretomes, little is known about how cancer-promoting secretomes are induced in CAFs. Only recently has it been reported that the transmembrane receptors of transforming growth factor- $\beta$  (TGF- $\beta$ ) and interleukin-1 (IL-1) induce in CAFs the production of immunomodulating secretomes and formation of a matrix-producing contractile phenotype [11,12]. The finding that the IL-1 receptor (IL-1R) in CAFs can regulate therapy resistance in rectal cancer prompted the idea that these receptors may serve as targets for stromal cell-directed therapy [13].

The adhesion molecule with Ig like domain 2 (AMIGO2; syn.: amphoterin-induced gene and ORF 2) is a type I transmembrane protein [14]. The protein was identified together with AMIGO3 in a search for proteins homologous to AMIGO1, which was detected in the same study by a screen for proteins induced in neurons by the neurite-promoting protein amphoterin [also known as high mobility group box 1 (HMGB1)] [14]. The similarity at the amino acid level between AMIGO2 and AMIGO1 or AMIGO3 is 48%, respectively [14]. All three proteins exhibit a similar structure, which harbors an N-terminal extracellular part of six leucine-rich repeats (LRRs) flanked by cysteine-rich LRR domains (LRRCT domain) and closest to the transmembrane domain, an Ig domain [14]. These motifs define the AMIGOs as members of both the Ig and the LRR super-families. Different signaling motifs are present on the intracellular part of AMIGO2. These include a consensus sequence for the casein kinase II serine/threonine kinase, four possible casein kinase I phosphorylation sites [14], a phosphoinositide-3-kinase (PI3K)-3-phosphoinositide-dependent protein kinase-1 (PDK1)-protein kinase B (Akt) activation motif [15], and a binding motif for the pseudokinase protein tyrosine kinase (PTK) 7 [16]. The presence of these motifs indicates that AMIGO2 may exert signaling activity.

Several previous studies reported that AMIGO2 plays a role in cancer, but these studies exclusively investigated its role when expressed in tumor cells [17–25]. For example, knockdown of the *AMIGO2* gene decreased

proliferation, invasion and adhesion to liver endothelial cells, whereas overexpression accelerated these processes in CRC cell lines [17,18,22]. Moreover, AMIGO2 can inhibit cisplatin-induced activation of apoptotic caspases in non-small cell lung cancer (NSCLC) cells [26].

As yet, no study has investigated the role of AMIGO2 in CAFs. We found that in CRC tissues, AMIGO2 is significantly higher expressed in CAFs compared to tumor cells and to normal tissue-associated fibroblasts (NAFs) resident in the healthy colon. AMIGO2 expression in CAFs was associated with a higher T-category and progressed, metastatic Union for International Cancer Control (UICC) stages. In agreement with this, *AMIGO2* expression was significantly higher in primary tumors of female patients, who frequently suffer from a more aggressive course of the disease compared to males [27]. Notably, CAFs and NAFs of the respective patients in culture maintained the differential AMIGO2 expression observed in the tissues. This enabled functional analyses of AMIGO2-dependent paracrine effects from CAF secretomes on CRC tumor cells. These studies demonstrated that AMIGO2 expression in CAFs induced the release of secretomes, which paracrine activate CRC tumor cell proliferation and migration. Our findings establish AMIGO2 as a new receptor-like protein that regulates the secretory phenotype of CAFs in a clinically relevant manner. Accordingly, AMIGO2 may serve as a new molecular target for stromal cell-directed therapy of CRC.

## Materials and methods

### Study approval

Approval for all studies involving patients was obtained from the ethics committee (Institutional Review Board) of the Universitätsklinikum Erlangen (approval number: 3914, Polyprobe study). Every participant received personal information and provided written informed consent for his/her involvement in this study. Patient data were pseudonymized, and all analyses were conducted in adherence to the principles outlined in the Declaration of Helsinki.

### Cell culture

NAFs and CAFs were extracted from CRC patients following a standardized, previously published protocol [5]. Fibroblasts were cultured in DMEM (Catalogue No. 21969, Gibco, Waltham, MA, USA) supplemented with 10% FCS (Sigma-Aldrich, St. Louis, MO, USA, Catalogue No. s0615, Kawasaki-shi, Kanagawa 215-0033 Japan), 1% L-glutamine (Thermo Fisher Scientific, Waltham, MA, USA, Catalogue No. 25030-024), and 1% penicillin/streptomycin stock solution (Gibco, Catalogue No. 15140-122) at 37 °C, with 8.5% CO<sub>2</sub> and 95% humidity.

The CRC cell lines SW480 and DLD-1 were purchased from the German Collection of Microorganisms

and Cell Cultures GmbH (DSMZ, ACC 313, Braunschweig, Germany, [RRID:CVCL\\_0546](#)) and the American Type Culture Collection (ATCC, CCL-221, [RRID:CVCL\\_0248](#), Manassas, VA, USA), respectively. CRC cell lines were cultured in Roswell Park Memorial Institute (RPMI) 1640 medium (Gibco, Cat:31870) supplemented with 10% FCS (Sigma Aldrich, Catalogue No. s0615) at 37 °C with 5% CO<sub>2</sub> and 95% humidity.

All cell cultures were tested regularly for mycoplasma contamination using the MycoAlert Mycoplasma Detection Kit (Catalogue No. LT07-701, Lonza, Basel, Switzerland) and were only used when found negative. Cell lines were regularly authenticated using short tandem repeat profiling [28].

## Tissues

Human CRC tissues were retrieved as formalin-fixed paraffin-embedded (FFPE) blocks after completion of routine diagnostics as retrospective study cohorts from the Institute of Pathology at the Friedrich-Alexander-Universität (FAU) Erlangen-Nürnberg, or from a proprietary cohort, which was prospectively enrolled between 2009 and 2012 at the Universitätsklinikum Erlangen. The inclusion criteria for all cohorts involved patients with a confirmed histological diagnosis of CRC UICC stages I to IV [29]. Exclusion criteria encompassed patients with hereditary tumors [hereditary nonpolyposis colorectal cancer (HNPCC), familial adenomatous polyposis (FAP)] or tumors arising from inflammatory bowel disease (ulcerative colitis, Crohn's disease). Detailed patient characteristics of the different cohorts are provided in supplementary material, Tables S1–S5.

## Immunohistochemistry

Immunohistochemical staining was conducted on FFPE samples of CRC and normal colon tissues. Tissue sections (4 µm) were deparaffinized, rehydrated, and subjected to antigen retrieval procedure at pH 6.1 (Catalogue No. S1699, Dako Cytomation, Glostrup, Denmark) and 95 °C for 20 min. Blocking of endogenous peroxidase was achieved with 7.5% H<sub>2</sub>O<sub>2</sub> for 10 min (Sigma Aldrich, Catalogue No. 1.0721.0250), followed by Avidin/Biotin (Catalogue No. SP-2001, Vector Laboratories, Newark, CA, USA) and 2.5% horse serum blocking (Vector Laboratories, Catalogue No. 30022) for 20 min. Mouse IgA anti-AMIGO2 (Catalogue No. sc-373699, [RRID:AB\\_10920216](#), 1:2,000, Santa Cruz Biotechnology, Dallas, TX, USA) and rabbit IgG anti-Vimentin (Catalogue No. ab92547, [RRID:AB\\_10562134](#), 1:30,000, Abcam, Cambridge, UK) were used as primary antibodies applied overnight at 4 °C. Respective isotype antibodies were used as controls [mouse IgA Isotype Control (S107), Thermo Fisher Scientific, Catalogue No. 14-4762-81, [RRID:AB\\_470125](#); rabbit polyclonal IgG, Cat# AB-105-C, [RRID:AB\\_354266](#), R&D Systems, Minneapolis, MN, USA]. Primary antibody binding was detected using the

Vectastain Elite ABC-Kit (Vector Laboratories, Catalogue No. PK-7200, [RRID:AB\\_2336828](#)) following the manufacturer's instructions. NovaRED (Vector Laboratories, Catalogue No. SK-4800, [RRID:AB\\_2336845](#)) was used as chromogen for 20 min, and afterward slides were counterstained with hematoxylin (Catalogue No. 1.05174.0500, Merck, Rahway, NJ, USA) for 1.5 min and then mounted with mounting medium (Vector Laboratories, Catalogue No. H-5000). Tile scans were performed for each slide using an Aperio VERSA 8 Slide Scanner (Leica Biosystems, Wetzlar, Germany) and analyzed using Aperio ImageScope Software version 12.4.3.7001 from Leica Biosystems. The average signal intensity in stromal areas was evaluated in six random locations per slide using ImageJ, undergoing analysis for integrated optical density (IOD) and area.

## Statistical analyses

For data with a normal distribution, statistical analysis for pairwise comparisons employed a two-tailed unpaired or paired Student's *t*-test. Non-normally distributed data were analyzed using a two-tailed Mann–Whitney *U*-test. Pearson's correlation coefficient and test were used to assess data correlation. All analyses were conducted using GraphPad Prism software version 8.00 ([RRID:SCR\\_002798](#), GraphPad Software, Boston, MA, USA). Statistical differences were determined through a two-tailed Student's *t*-test,  $\chi^2$  test, or ANOVA, followed by *post hoc* analysis using SPSS version 21 (IBM, [RRID:SCR\\_002865](#)), as outlined in the figure legends. *p* values below 0.05 were considered significant, and error bars in all graphs indicate  $\pm$  SD. The impact of sex as a biological variable on tumor aggressiveness was considered.

Further materials and methods are given in Supplementary materials and methods.

## Results

AMIGO2 expression is increased in cultivated CAFs compared to NAFs, consistent with originating tissues

NAFs and CAFs were isolated and cultivated from primary tumor tissues of CRC following previously described protocols [5]. The isolated cells exhibited a spindle-shaped morphology, expressed vimentin, and were negative for markers of epithelial cells (CK-20) and hematopoietic cells (CD45), which confirmed their fibroblast identity [5]. Comparative transcriptome analyses of CAFs (*n* = 6) and NAFs (*n* = 3) with RNA sequencing (RNA-seq) and subsequent screening for differentially expressed membrane proteins revealed that the expression of the type 1 transmembrane protein *AMIGO2* was significantly increased in CAFs compared to NAFs (Figure 1A). This result was confirmed by reverse transcription quantitative polymerase chain



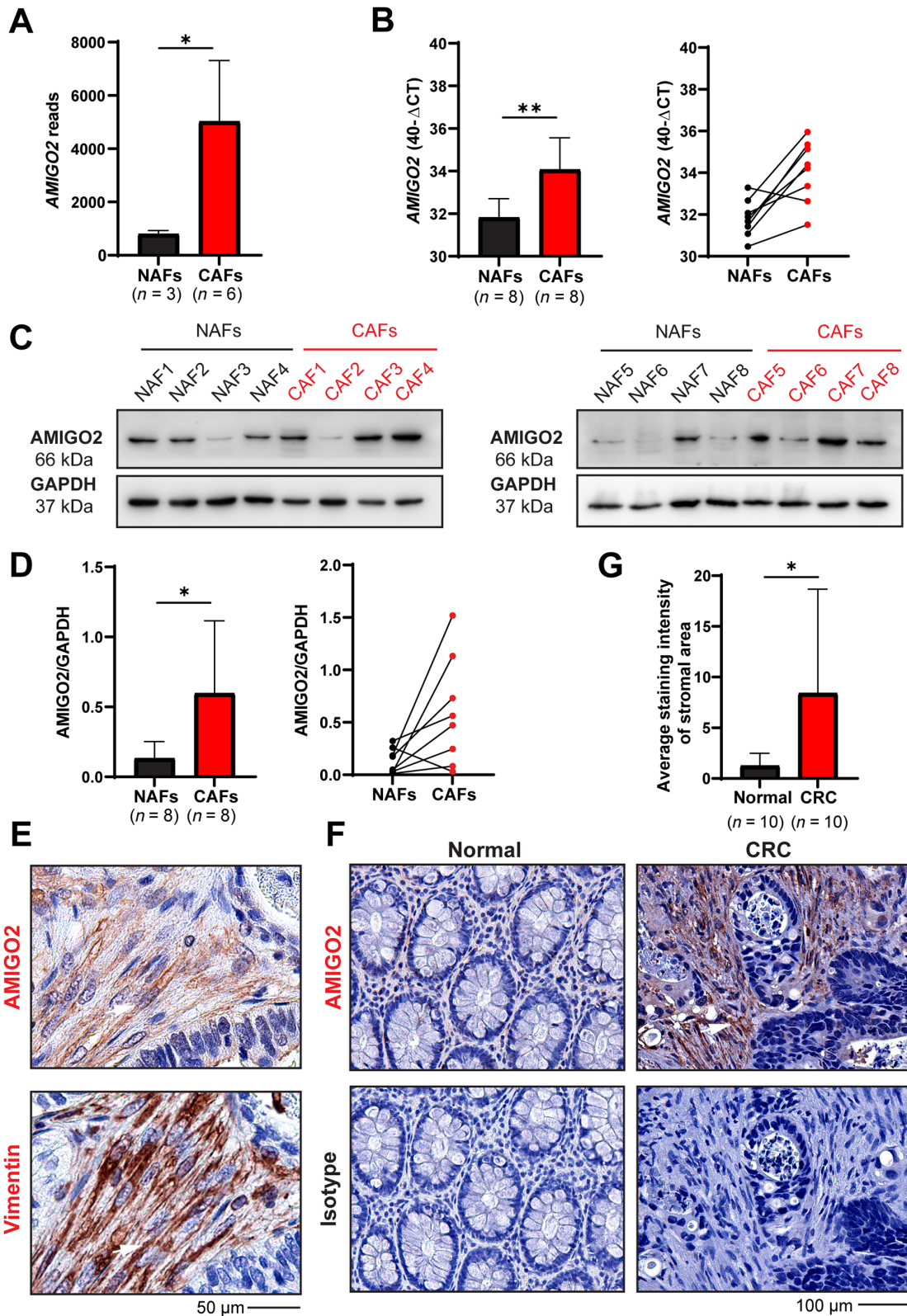


Figure 1. AMIGO2 is upregulated in CAFs compared to NAFs. (A) *AMIGO2* reads from bulk RNA-seq of normal tissue-associated fibroblasts (NAFs) and CAFs isolated from CRC patients. Results are given as mean  $\pm$  SD of read values. A two-tailed unpaired Student's *t*-test was used for statistical evaluation (\**p* = 0.0175). (B) Comparison of *AMIGO2* mRNA expression in paired NAFs and CAFs from the same patients (*n* = 8) each. *RPL37A* was used as a reference transcript for normalization. Results are given as 40 -  $\Delta$ Ct (Ct-*AMIGO2* - Ct-*RPL37A*) (mean  $\pm$  SD, *t*-test, \*\**p* = 0.0025). (C) *AMIGO2* western blot of paired NAFs and CAFs from the same patients as in (B). GAPDH was used as a loading control. (D) Quantitative evaluation of western blot results from (C). Results are shown as mean  $\pm$  SD (*t*-test, \*\**p* = 0.0267, left) or by pairwise comparison for each patient (right). (E) Staining for *AMIGO2* and the fibroblast marker vimentin in consecutive tissue sections of human CRC tissues. Double-positive fibroblasts are indicated by white arrows. (F) *AMIGO2* immunohistochemistry on normal and CRC tissues (*n* = 10). Patient 1 images are also used in supplementary material, Figures S2. (G) Quantification of stromal staining intensity between normal and CRC tissues (mean  $\pm$  SD, two-tailed, unpaired Student's *t*-test, \**p* < 0.05).



reaction (RT-qPCR) in additional NAF and CAF cultures, which were established from normal colon and corresponding tumor tissue of the same patients, respectively ( $n = 8$ ) (Figure 1B, left). *AMIGO2* expression was increased in CAFs compared to NAFs in all patients except one (Figure 1B, right). Increased *AMIGO2* expression in CAFs was confirmed at the protein level using western blotting (Figure 1C). Pairwise comparison of normalized signal intensities of *AMIGO2* protein in CAFs and corresponding NAFs from the same patients revealed a significant increase in CAFs in 75% of the patients (Figure 1D). The immunization peptide used for generation of the *AMIGO2* antibody exhibited less than 50% identical amino acids (13 of 30) with the corresponding regions in *AMIGO1* and *AMIGO3* (supplementary material, Figure S1). Accordingly, it is unlikely that the two other variants were detected by the antibody, in contrast to what was suggested by Goto *et al* [30].

In CRC tissues, staining for *AMIGO2* and the fibroblast marker vimentin on consecutive sections demonstrated that *AMIGO2* was expressed predominantly in fibroblasts (Figure 1E, white arrows), whereas tumor cells showed either low or absent expression. Concordant with the results obtained in cultivated fibroblasts, *AMIGO2* expression was higher in CAFs in the stroma of CRC tissues compared to fibroblasts in normal tissues of the same patients (Figure 1F and supplementary material, Figure S2,  $n = 10$ ; patient characteristics are shown in supplementary material, Table S1). Quantitative analyses confirmed a significant increase of *AMIGO2* expression in CAFs in CRC (Figure 1G). Tile scans of large tissue sections presenting both tumor tissue and tissue with normal healthy morphology confirmed in the same sections that *AMIGO2* expression is clearly higher in CAFs (supplementary material, Figure S3, red frame) compared to NAFs (supplementary material, Figure S3, blue frame). Of note, also in these experiments, *AMIGO2* expression in the CRC tumor cells was low or absent (supplementary material, Figure S3).

*AMIGO2* expression in CAFs is induced by TGF- $\beta$ , higher in females and increased in advanced UICC stages in CRC

To determine the disease-related expression of *AMIGO2*, a prospectively collected cohort of CRC patients ( $n = 338$ ) was analyzed using Taqman RT-qPCR using RNA extracted from FFPE tissues of primary tumors (supplementary material, Table S2). *AMIGO2* expression increased with tumor size (T-category) (Figure 2A), lymph node metastasis (N-category) (Figure 2B), and distant metastasis (M-category) (Figure 2C). No difference was observed between the individual non-metastatic tumor stages (UICC I versus II) or between tumors with locoregional and distant metastasis (UICC III versus IV) (Figure 2D). However, *AMIGO2* expression was significantly increased between non-metastatic UICC stages (UICC I or II) and metastatic stages (UICC III or IV) (Figure 2D). Of note, *AMIGO2* expression was not associated with tumor grading (supplementary material, Figure S4).

To investigate which factor/s in the CRC-TME might be responsible for the increased *AMIGO2* expression in CAFs, we stimulated NAFs with IL-17 $\alpha$ , TNF- $\alpha$ , and TGF- $\beta$ . All three factors are involved in the pathogenesis of CRC [31–33]. In addition, IL-17 $\alpha$  and TNF- $\alpha$  have been shown to stimulate *AMIGO2* expression in synovial fibroblasts in rheumatic arthritis [34]. TGF- $\beta$  treatment significantly increased *AMIGO2* expression in NAFs, whereas no effect was observed with IL-17 $\alpha$  and TNF- $\alpha$ , either singly or combined (Figure 2E).

In addition, *AMIGO2* expression was significantly increased in females compared to males in the total cohort (Figure 2F). The gender-related difference was further increased when exclusively metastatic UICC IV stages were compared (Figure 2G). Notably, females frequently suffer from a more aggressive course of the disease compared to males [27]. The different tumor stages were similarly distributed in the male and female groups and can be excluded as the reason for the gender-associated difference in *AMIGO2* expression (Figure 2H). Analysis of *AMIGO2* expression at the protein level using immunohistochemistry in nonmetastatic (UICC I) and metastatic (UICC IV) CRC tissues ( $n = 24$ ) (supplementary material, Table S3, patient characteristics) and subsequent quantitative signal analyses confirmed that *AMIGO2* was significantly higher expressed in the metastatic tumor stages (Figure 2I,J).

CAF-associated *AMIGO2* expression is highest in tissues of CRC-derived liver metastases and associated with poor patient survival

Analyses of *AMIGO2* expression levels in tissues of CRC-derived liver metastases identified increased levels in CAFs in the metastatic tissues compared to the primary tumors (Figure 3A,B and supplementary material, Figure S5). The increased *AMIGO2* expression in the metastatic tissues was uniformly detected in all patients examined [Figure 3B, right; supplementary material, Table S4 (patient characteristics)]. Most importantly, *AMIGO2* expression in CAFs of the primary tumors was associated with a significantly reduced overall survival in The Cancer Genome Atlas-colon adenocarcinoma (TCGA-COAD) cohort of human colon tumor patients (Figure 3C,  $n = 136$ ) and with a significantly reduced cancer-related survival in our own prospectively collected cohort of colon cancer patients ( $n = 254$ ) [Figure 3D and supplementary material, Table S5 (patient characteristics)].

Overexpression of *AMIGO2* in NAFs induces tumor-activating secretomes

In the next step, we investigated how *AMIGO2* expression in CAFs may contribute to CRC tumorigenesis. *AMIGO2* is a type 1 membrane protein and may be released from CAFs due to proteolytic processing or by cell death. Following this hypothesis, we looked for the presence of *AMIGO2* in cell culture supernatants of *AMIGO2*-positive cells using ELISA. No evidence for

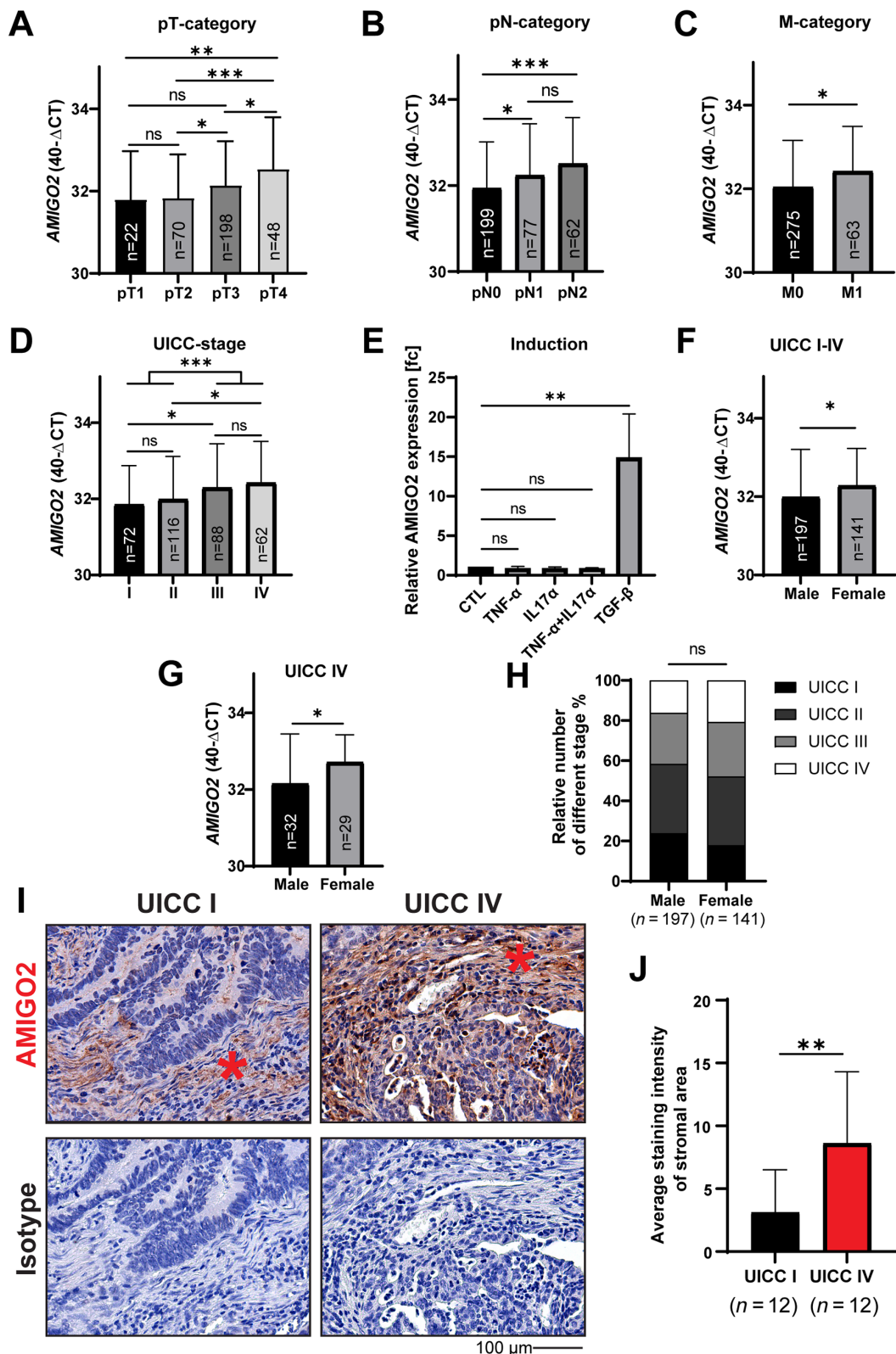
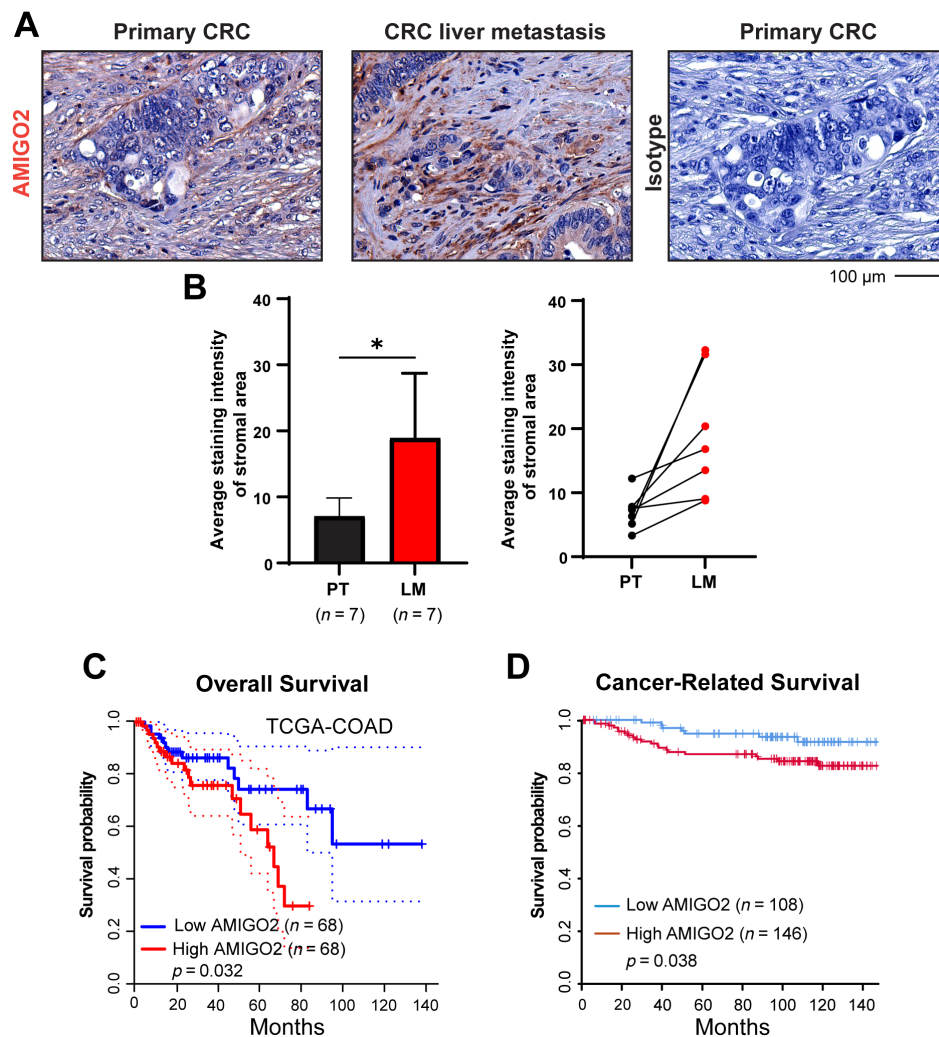


Figure 2. AMIGO2 expression is induced by TGF-β and increased in metastatic stages of CRC and female patients. AMIGO2 mRNA expression in CRC primary tumors of a prospectively collected cohort (n = 338) in relation to (A) tumor size (T-category), (B) lymph node metastasis (N-category), (C) distant organ metastasis (M-category), and (D) different Union for International Cancer Control (UICC) stages. (E) NAF cultures from different CRC patients (n = 3) were treated with IL-17α (0.5 ng/ml), TNF-α (50 ng/ml), TGF-β (5 ng/ml), and combined IL-17α and TNF-α for 24 h, and subsequently AMIGO2 expression was determined by RT-qPCR. Results are given in fold-change (mean ± SD, t-test, \*\*p = 0.0058). Comparison of AMIGO2 mRNA expression between male and female patients in (F) the total cohort from above and (G) patients with distant metastases (UICC IV). (H) UICC stage distributions in male and female patients from the cohort above (χ<sup>2</sup> test). (I) Immunohistochemical detection of AMIGO2 in non-metastatic (UICC I) and metastatic stages (UICC IV) of CRC (n = 12). Fibroblasts in the stroma are indicated by asterisks. (J) Quantification of stromal fibroblast staining intensity from the results obtained in (I). Results are shown as mean ± SD (two-tailed, unpaired Student's t-test, \*\*p < 0.001).



**Figure 3.** AMIGO2 expression is increased in CRC-derived liver metastasis and is associated with poor patient survival. (A) Detection of AMIGO2 expression in primary tumors (PTs) and corresponding liver metastases (LMs) of the same patients ( $n = 7$ ) using immunohistochemistry. These images are from patient 34 – depicted in the supplementary material, Figure S5. (B) Quantitative comparison of results from (A) (mean  $\pm$  SD, two-tailed unpaired Student's  $t$ -test,  $*p < 0.05$ , left) and pairwise comparison of AMIGO2 expression in PT and LM in each patient (right). (C) Overall survival of patients with colon carcinoma (TCGA-COAD cohort) with high (red,  $n = 68$ ) and low (blue,  $n = 68$ ) AMIGO2 mRNA expression (Kaplan–Meier plot,  $p = 0.032$ ). (D) Cancer-related survival in a prospectively collected cohort of patients with CRC with high (red,  $n = 146$ ) and low (blue,  $n = 108$ ) AMIGO2 mRNA expression (Kaplan–Meier plot,  $p = 0.038$ ).

the presence of AMIGO2 in the conditioned media (CM) of two CAF cultures with the highest AMIGO2 expression was obtained by an ELISA with a sensitivity of 0.2 pg/ml (data not shown). This result suggested that AMIGO2 was not released from CAFs and did not act directly on tumor cells. Alternatively, AMIGO2 in fibroblasts may exert pathogenic functions by inducing the release of secretomes that activate the tumor cells in a paracrine manner. To address this idea, AMIGO2 was overexpressed in NAFs by transient transfection, CM of the cells were harvested, and their effects on CRC cell proliferation and migration were analyzed (Figure 4A). After transfection with the AMIGO2 expression plasmid, AMIGO2 expression was strongly increased in NAFs in comparison to control plasmid-transfected NAFs (Figure 4B). CM of AMIGO2-overexpressing fibroblasts significantly stimulated the proliferation of two different CRC cell lines (Figure 4C, SW480, DLD1). Similarly,

the migration of the respective cancer cells was significantly activated by CM obtained from AMIGO2-overexpressing fibroblasts (Figure 4D,E).

#### Inhibition of AMIGO2 expression in CAFs abandons tumor-activating secretomes

To investigate whether the absence or reduction of AMIGO2 expression in CAFs can reduce the tumor cell-activating capacity of the corresponding secretomes, AMIGO2 expression in CAFs was inhibited using siRNA, and the impact of the corresponding CM was investigated on CRC tumor cell lines (Figure 5A). Comparison of three different siRNAs showed that siRNA C had the strongest inhibitory effect on AMIGO2 expression (Figure 5B left). This was confirmed by quantitative evaluation of band intensity (Figure 5B right). CM harvested from siRNA C-transfected CAFs activated



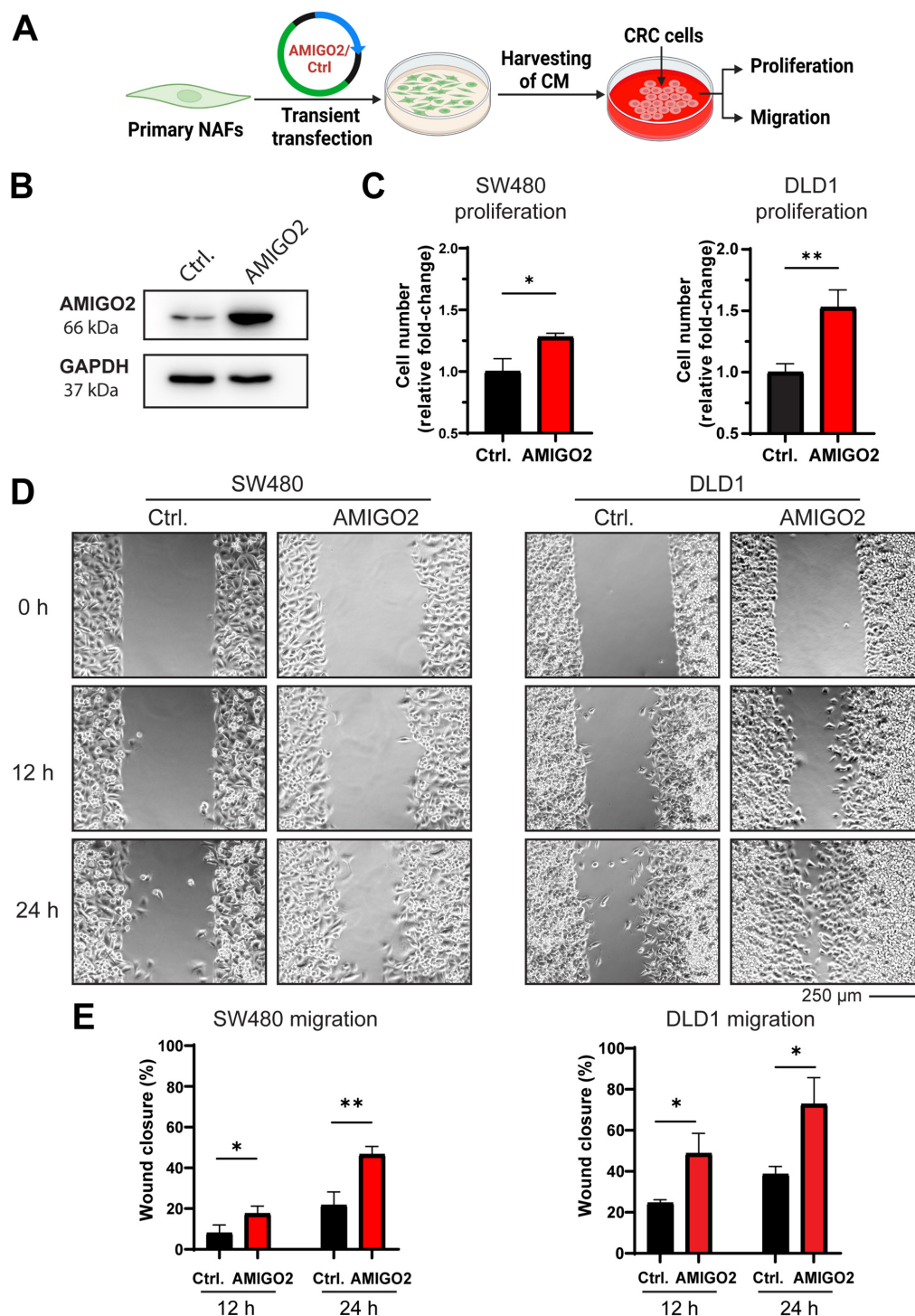


**Figure 4.** AMIGO2 overexpression in NAFs promotes proliferation and migration of CRC tumor cells. (A) An expression plasmid of AMIGO2 cDNA or the respective control vector without AMIGO2 were transfected into NAFs, CM were harvested, and their impact on proliferation and migration of two different CRC tumor cell lines was tested (SW480, DLD1). Created with Biorender.com. (B) Western blot for AMIGO2 expression after transfection of NAFs. GAPDH is shown as a loading control. (C) CM of AMIGO2-transfected NAFs enhanced proliferation of SW480 (left) and DLD1 (right) cells. (D) CM of AMIGO2-transfected NAFs promoted migration of SW480 (left) and DLD1 (right) cells. (E) Quantitative evaluation of the results obtained in (D) after 12 and 24 h of incubation with CM. Mean  $\pm$  SD. Two-tailed unpaired Student's *t*-test was used to determine statistical significance (\* $p < 0.05$ , \*\* $p < 0.001$ ).

proliferation of two different CRC cell lines significantly lower compared to CM obtained from scrambled siRNA-transfected control cells (Figure 5C). Similarly, the CM obtained from CAFs with decreased AMIGO2 expression had a significantly reduced effect on the stimulation of

migration of the CRC cell lines (Figure 5D,E). Taken together, these results indicate that AMIGO2 expression in CAFs is both necessary and sufficient for the release of secretomes that activate the proliferation and migration of tumor cells in a paracrine manner.

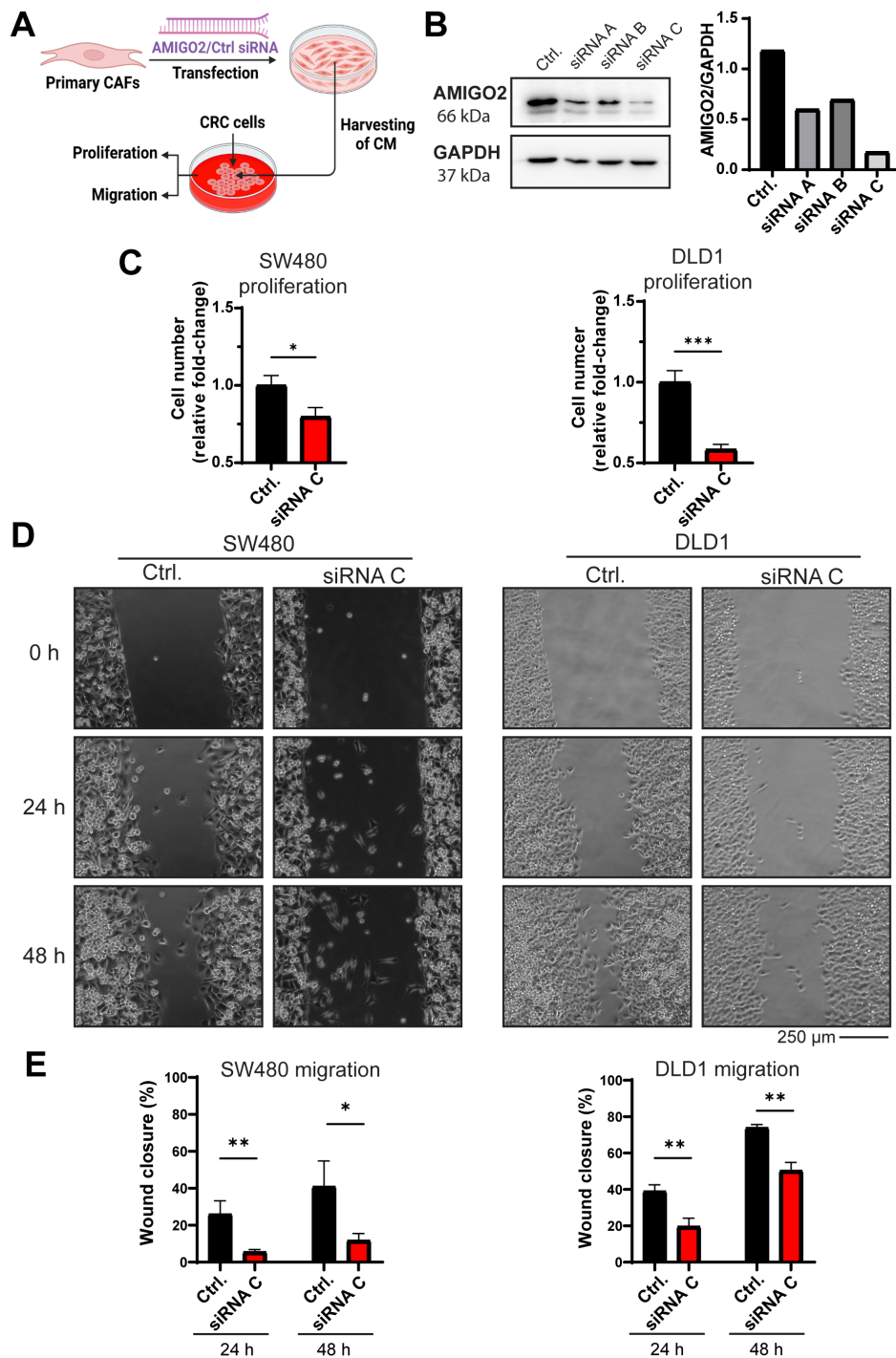


**Figure 5.** siRNA-mediated inhibition of AMIGO2 expression in CAFs reduces CM effects on tumor cell proliferation and migration. (A) siRNA targeting specifically *AMIGO2* or a scrambled control siRNA were transfected into CAFs, CM were harvested, and their impact on proliferation and migration of two different CRC tumor cell lines was tested (SW480, DLD1). Created with Biorender.com. (B) Western blot for AMIGO2 expression and GAPDH as a loading control after transfection of CAFs with three different AMIGO2-siRNAs (left). Quantitative results of AMIGO2 signals in relation to GAPDH are shown (right). (C) CM of CAFs transfected with AMIGO2-siRNA C or a control-siRNA were harvested and used in proliferation experiments with SW480 (left) and DLD1 (right) cells. (D) CM of CAFs transfected with AMIGO2-siRNA C or a control-siRNA were harvested and used in migration experiments with SW480 (left) and DLD1 (right) cells. (E) Quantitative evaluation of the results obtained in (D) after 24 and 48 h of incubation with CM. Mean  $\pm$  SD. Two-tailed unpaired Student's *t*-test was used to determine statistical significance (\**p* < 0.05, \*\**p* < 0.001).

## Discussion

Different cell types communicate in the TME through a broad panel of various secreted factors, which are part of the cellular secretomes. The interactions of CAFs with

tumor cells are of paramount importance in the pathogenesis of CRC [13]. CAFs release many different cytokines (IL-1, IL-6, IL-11, IL-17, IL-33), growth factors [TGF- $\beta$ , hepatocyte growth factor (HGF)], chemokines (CXCL1, CXCL2, CXCL12), non-coding RNAs, matrix

proteinases (MMP2, MMP9, MMP14), and ECM components (collagen I, collagen VI), many of which can activate tumor cells and/or contribute to an increase in the aggressiveness of the disease [7–10,35–37]. In contrast to the many proteins secreted from CAFs in CRC, relatively little is known about what regulates the production of different secretomes in CAFs. Only recently, TNF-receptor and IL-1 receptor were identified to regulate the release of different secretomes from CAFs [11–13]. Specifically, the IL-1R has been shown to regulate therapy resistance by an IL-1-dependent paracrine activity released from CAFs [13]. Against this background, the specific goal of this study was to search for further membrane-bound molecules in CAFs that may regulate the release of tumor-activating secretomes in these cells. Membrane-bound receptor-like molecules were chosen as preferred targets, as these molecules may regulate CAF secretomes in response to the extracellular TME.

We found that cultivated CAFs from CRC expressed the type 1 membrane protein AMIGO2 significantly more highly compared to NAFs isolated from normal colon of the same patients in seven of eight cases (87.5%). Notably, differential AMIGO2 expression in CAFs and NAFs was confirmed in CRC tissues, where AMIGO2 expression in CAFs correlated with larger tumor size, lymph node metastasis, and progressed tumor stages. It is of specific interest that AMIGO2 expression was higher in female patients, who are generally known to exhibit a more aggressive course of the disease compared to male patients. This observation clearly supports the association of high AMIGO2 expression levels with aggressive CRC [27]. In agreement with these findings, elevated AMIGO2 expression was associated with reduced overall and cancer-related survival in different cohorts of CRC patients.

A putative role of AMIGO2 in CRC was previously investigated, but all of these studies exclusively focused on its expression in tumor cells [17–25]. Experimentally induced upregulation or inhibition of AMIGO2 expression activated or inhibited proliferation and migration of these cells, respectively [17,18,22]. Our findings suggest that AMIGO2 may be more relevant in CAFs because AMIGO2 expression in CRC tissues was significantly higher in CAFs compared to tumor cells. This finding was carefully validated in our study using a variety of different experiments: (1) expression results on AMIGO2 were identically reproduced, both at the RNA and protein levels; (2) each immunohistochemical staining was controlled with an isotype antibody staining, which was negative; (3) in tile scans of large areas of tissue, it was confirmed on the same slide that AMIGO2 expression was higher in CAFs compared to NAFs and to adjacent tumor cells; (4) AMIGO2 expression was higher in cultivated CAFs than in NAFs, and the same result was obtained at the tissue level when NAFs resident in normal colon tissues and CAFs in CRC tumor tissue of the same patients were investigated; (5) the immunization peptide used for generation of the AMIGO2 antibody exhibited only low homology to the respective peptide sequences in AMIGO1 and AMIGO3; (6) furthermore, overexpression

of AMIGO2 in cultured fibroblasts increased and, conversely, specific inhibition of AMIGO2 expression decreased the signal obtained with the anti-AMIGO2 antibody in western blot analyses. The latter approach also confirmed that the antibody detected specifically AMIGO2 because the siRNA against AMIGO2 did not bind to AMIGO1 and AMIGO3 but almost fully suppressed the signal obtained in CAFs by western blotting (siRNA C, Figure 5B, right); (7) moreover, RNA-seq-based comparison of CAF and NAF transcriptomes only detected AMIGO2, suggesting that this was the predominant member of the AMIGO family expressed in CAFs. Altogether, these manifold controls confirmed concordantly that AMIGO2 was predominantly expressed in CAFs of CRC.

Cancer fibroblasts are a highly plastic cell type. Accordingly, it is likely that AMIGO2 expression in CAFs is induced by TME-dependent external stimulation. In agreement with this hypothesis, we found that TGF- $\beta$  highly and significantly induced AMIGO2 expression in NAFs. TGF- $\beta$  is associated with worse prognosis in CRC patients [32,38] and has been reported recently to act as a key cytokine in hepatic colonization by affecting tumor cells, as well as tumor stroma, vasculature, and immune cells [39]. These findings indicate that TGF- $\beta$  may be an important inducer of the increased AMIGO2 expression in CAFs, in both CRC primary lesions and metastases. Moreover, AMIGO2 expression can be induced in melanoma cells by bromodomain and extraterminal domain (BET) proteins, which regulate gene transcription through epigenetic interactions [16,40]. Interestingly, we recently showed that epigenetic imprinting was an important regulatory pathway in CRC fostering in cultivated stromal cells, in this case endothelial cells, the maintenance of tumor-associated deregulation of gene expression in culture [41,42]. Alternatively, AMIGO2 may be induced by HMGB1, which is associated with poorer outcomes and therapeutic responses in many tumors, including CRC [43], and was shown to induce its homolog AMIGO1 [14]. Based on these considerations, it is likely that AMIGO2 expression in CAFs may be induced in the process of a cellular response to the TME in CRC. Our results suggest that TGF- $\beta$  may be involved in this TME-dependent activation.

AMIGO2 may regulate the production and release of tumor-promoting secretomes in CAFs via several signaling motifs detected in its intracellular domain. Of these, Akt activation is of highest interest, because the absence of AMIGO2 in endothelial cells deactivated Akt and induced apoptosis in these cells, demonstrating that AMIGO2 can act on Akt in mesenchymal cells [15]. Most interestingly, Akt has been involved in the regulation of secretion of different proteins, including insulin [44] and IL-6 [45], and has been shown to regulate secretome changes in drug-sensitive cancer cells [46]. Specifically, the latter further supports our observation that AMIGO2 regulates the appearance of tumor-promoting secretomes in CAFs.

In conclusion, we have determined that the transmembrane protein AMIGO2 regulates in CAFs the release of tumor-promoting secretomes in a clinically relevant



manner. AMIGO2 expression was sufficient to induce in NAFs the release of a tumor-activating CAF secretome, and conversely, the inhibition of AMIGO2 in CAFs was sufficient to revert the CAF secretome to a NAF-like secretome with lower tumor-promoting activity. Based on this, AMIGO2 may serve as a new target for tailored therapy approaches to interfering with CAF tumor cell communication in CRC.

## Acknowledgements

Yongsong Yong was sponsored by a MD doctoral scholarship from Xinghua People's Hospital Affiliated to Yangzhou University, Taizhou, Jiangsu, PR China. The present work was performed in (partial) fulfillment of the requirements for obtaining the degree Doctor of Medicine for first author Yongsong Yong. The work of the authors was supported by grants from the German Research Foundation (DFG) FOR 2438, subproject 2 (project ID 280163318) to Elisabeth Naschberger/Michael Stürzl; by DFG SFB/TRR 241, subproject A06 (project ID 375876048) to Michael Stürzl; by DFG STU 238/10-1 (project ID 437201724) to Michael Stürzl; by DFG TRR 305, subproject B08 (project ID 429280966) to Elisabeth Naschberger; by DFG-NOTICE program (project ID 493624887) to Elisabeth Naschberger; by W. Lutz Stiftung to Michael Stürzl; and by Forschungstiftung Medizin am Universitätsklinikum Erlangen to Michael Stürzl.

## Author contribution statement

EN, MS and YY designed the experiments. EN, RD, VSS and YY performed the experiments. EN, MS, RD, SM, TZ, YY and YZ analyzed the data. BAZ, CF, CIG, EN, KP, MS, QF, TG, TZ and YZ provided key reagents, materials, analysis tools and helpful ideas. MS provided resources. EN and MS acquired funding. EN and MS supervised the experiments. EN, MS and YY wrote the manuscript. All authors approved the final version of the manuscript.

## Data availability statement

The data generated in this study are available upon request from the corresponding author. The Bulk RNA-seq data have been deposited at ArrayExpress under Accession Number E-MTAB-14208.

## References

- Hanahan D, Weinberg RA. Hallmarks of cancer: the next generation. *Cell* 2011; **144**: 646–674.
- Guinney J, Dienstmann R, Wang X, et al. The consensus molecular subtypes of colorectal cancer. *Nat Med* 2015; **21**: 1350–1356.
- Kalluri R. The biology and function of fibroblasts in cancer. *Nat Rev Cancer* 2016; **16**: 582–598.
- Bhowmick NA, Neilson EG, Moses HL. Stromal fibroblasts in cancer initiation and progression. *Nature* 2004; **432**: 332–337.
- Schellerer VS, Langheinrich M, Hohenberger W, et al. Tumor-associated fibroblasts isolated from colorectal cancer tissues exhibit increased ICAM-1 expression and affinity for monocytes. *Oncol Rep* 2014; **31**: 255–261.
- Chen Y, McAndrews KM, Kalluri R. Clinical and therapeutic relevance of cancer-associated fibroblasts. *Nat Rev Clin Oncol* 2021; **18**: 792–804.
- Houthuijzen J, Jonkers J. Cancer-associated fibroblasts as key regulators of the breast cancer tumor microenvironment. *Cancer Metastasis Rev* 2018; **37**: 577–597.
- Augsten M. Cancer-associated fibroblasts as another polarized cell type of the tumor microenvironment. *Front Oncol* 2014; **4**: 62.
- Pickup M, Novitskiy S, Moses HL. The roles of TGF $\beta$  in the tumour microenvironment. *Nat Rev Cancer* 2013; **13**: 788–799.
- Kennel KB, Bozlar M, De Valk AF, et al. Cancer-associated fibroblasts in inflammation and antitumor immunity. *Clin Cancer Res* 2023; **29**: 1009–1016.
- Biffi G, Oni TE, Spielman B, et al. IL1-induced JAK/STAT signaling is antagonized by TGF $\beta$  to shape CAF heterogeneity in pancreatic ductal adenocarcinoma. *Cancer Discov* 2019; **9**: 282–301.
- Öhlund D, Handly-Santana A, Biffi G, et al. Distinct populations of inflammatory fibroblasts and myofibroblasts in pancreatic cancer. *J Exp Med* 2017; **214**: 579–596.
- Nicolas AM, Pesic M, Engel E, et al. Inflammatory fibroblasts mediate resistance to neoadjuvant therapy in rectal cancer. *Cancer Cell* 2022; **40**: 168–184.e13.
- Kuja-Panula J, Kiittomäki M, Yamashiro T, et al. AMIGO, a transmembrane protein implicated in axon tract development, defines a novel protein family with leucine-rich repeats. *J Cell Biol* 2003; **160**: 963–973.
- Park H, Lee S, Shrestha P, et al. AMIGO2, a novel membrane anchor of PDK1, controls cell survival and angiogenesis via Akt activation. *J Cell Biol* 2015; **211**: 619–637.
- Fontanals-Cirera B, Hasson D, Vardabasso C, et al. Harnessing BET inhibitor sensitivity reveals AMIGO2 as a melanoma survival gene. *Mol Cell* 2017; **68**: 731–744.e9.
- Kanda Y, Osaki M, Onuma K, et al. Amigo2-upregulation in tumour cells facilitates their attachment to liver endothelial cells resulting in liver metastases. *Sci Rep* 2017; **7**: 43567.
- Rabenau KE, O'Toole JM, Bassi R, et al. DEGA/AMIGO-2, a leucine-rich repeat family member, differentially expressed in human gastric adenocarcinoma: effects on ploidy, chromosomal stability, cell adhesion/migration and tumorigenicity. *Oncogene* 2004; **23**: 5056–5067.
- Huo T, Canepa R, Sura A, et al. Colorectal cancer stages transcriptome analysis. *PLoS One* 2017; **12**: e0188697.
- Nakamura S, Kanda M, Shimizu D, et al. AMIGO2 expression as a potential prognostic biomarker for gastric cancer. *Anticancer Res* 2020; **40**: 6713–6721.
- Liu Y, Yang J, Shi Z, et al. In vivo selection of highly metastatic human ovarian cancer sublines reveals role for AMIGO2 in intra-peritoneal metastatic regulation. *Cancer Lett* 2021; **503**: 163–173.
- Tanio A, Saito H, Amisaki M, et al. AMIGO2 as a novel indicator of liver metastasis in patients with colorectal cancer. *Oncol Lett* 2021; **21**: 278.
- Company V, Murcia-Ramón R, Andreu-Cervera A, et al. Adhesion molecule Amigo2 is involved in the fasciculation process of the fasciculus retroflexus. *Dev Dyn* 2022; **251**: 1834–1847.
- Goto K, Morimoto M, Osaki M, et al. The impact of AMIGO2 on prognosis and hepatic metastasis in gastric cancer patients. *BMC Cancer* 2022; **22**: 280.

25. Izutsu R, Osaki M, Jehung JP, *et al.* Liver metastasis formation is defined by AMIGO2 expression via adhesion to hepatic endothelial cells in human gastric and colorectal cancer cells. *Pathol Res Pract* 2022; **237**: 154015.
  26. Chen LK, Lin SP, Xie YH, *et al.* AMIGO2 attenuates innate cisplatin sensitivity by suppression of GSDME-conferred pyroptosis in non-small cell lung cancer. *J Cell Mol Med* 2023; **27**: 2412–2423.
  27. Cai Y, Rattray NJW, Zhang Q, *et al.* Sex differences in colon cancer metabolism reveal a novel subphenotype. *Sci Rep* 2020; **10**: 4905.
  28. Stürzl M, Gaus D, Dirks WG, *et al.* Kaposi's sarcoma-derived cell line SLK is not of endothelial origin, but is a contaminant from a known renal carcinoma cell line. *Int J Cancer* 2013; **132**: 1954–1958.
  29. Brierley JD, Gospodarowicz MK, Wittekind C. *TNM classification of malignant Tumours* (8th edn). Wiley-Blackwell, 2017.
  30. Goto K, Osaki M, Izutsu R, *et al.* Establishment of an antibody specific for AMIGO2 improves immunohistochemical evaluation of liver metastases and clinical outcomes in patients with colorectal cancer. *Diagn Pathol* 2022; **17**: 16.
  31. Wang K, Kim MK, Di Caro G, *et al.* Interleukin-17 receptor a signaling in transformed enterocytes promotes early colorectal tumorigenesis. *Immunity* 2014; **41**: 1052–1063.
  32. Busenhardt P, Montalban-Arques A, Katkeviciute E, *et al.* Inhibition of integrin  $\alpha v \beta 6$  sparks T-cell antitumor response and enhances immune checkpoint blockade therapy in colorectal cancer. *J Immunother Cancer* 2022; **10**: e003465.
  33. Oliver Metzger M, Fuchs D, Tagscherer KE, *et al.* Inhibition of caspases primes colon cancer cells for 5-fluorouracil-induced TNF- $\alpha$ -dependent necroptosis driven by RIP1 kinase and NF- $\kappa$ B. *Oncogene* 2016; **35**: 3399–3409.
  34. Benedetti G, Bonaventura P, Lavocat F, *et al.* IL-17A and TNF- $\alpha$  increase the expression of the antiapoptotic adhesion molecule Amigo-2 in arthritis synoviocytes. *Front Immunol* 2016; **7**: 254.
  35. Yan L, Zheng J, Wang Q, *et al.* Role of cancer-associated fibroblasts in colorectal cancer and their potential as therapeutic targets. *Biochem Biophys Res Commun* 2023; **681**: 127–135.
  36. Fang Z, Xu J, Zhang B, *et al.* The promising role of noncoding RNAs in cancer-associated fibroblasts: an overview of current status and future perspectives. *J Hematol Oncol* 2020; **13**: 154.
  37. Mishra D, Banerjee D. Secretome of stromal cancer-associated fibroblasts (CAFs): relevance in cancer. *Cells* 2023; **12**: 628.
  38. Fujishita T, Kojima Y, Kajino-Sakamoto R, *et al.* The cAMP/PKA/CREB and TGF $\beta$ /SMAD4 pathways regulate stemness and metastatic potential in colorectal cancer cells. *Cancer Res* 2022; **82**: 4179–4190.
  39. Marvin DL, Heijboer R, Ten Dijke P, *et al.* TGF- $\beta$  signaling in liver metastasis. *Clin Transl Med* 2020; **10**: e160.
  40. Taniguchi Y. The Bromodomain and extra-terminal domain (BET) family: functional anatomy of BET paralogous proteins. *Int J Mol Sci* 2016; **17**: 1849.
  41. Naschberger E, Fuchs M, Dickel N, *et al.* Tumor microenvironment-dependent epigenetic imprinting in the vasculature predicts colon cancer outcome. *Cancer Commun (Lond)* 2023; **43**: 1280–1285.
  42. Naschberger E, Liebl A, Schellerer VS, *et al.* Matricellular protein SPARCL1 regulates tumor microenvironment-dependent endothelial cell heterogeneity in colorectal carcinoma. *J Clin Invest* 2016; **126**: 4187–4204.
  43. Chen R, Zou J, Zhong X, *et al.* HMGB1 in the interplay between autophagy and apoptosis in cancer. *Cancer Lett* 2024; **581**: 216494.
  44. Bernal-Mizrachi E, Fatrai S, Johnson JD, *et al.* Defective insulin secretion and increased susceptibility to experimental diabetes are induced by reduced Akt activity in pancreatic islet beta cells. *J Clin Invest* 2004; **114**: 928–936.
  45. Cahill CM, Rogers JT. Interleukin (IL) 1beta induction of IL-6 is mediated by a novel phosphatidylinositol 3-kinase-dependent AKT/IkappaB kinase alpha pathway targeting activator protein-1. *J Biol Chem* 2008; **283**: 25900–25912.
  46. Obenauf AC, Zou Y, Ji AL, *et al.* Therapy-induced tumour secretomes promote resistance and tumour progression. *Nature* 2015; **520**: 368–372.
  47. Tang Z, Li C, Kang B, *et al.* GEPIA: a web server for cancer and normal gene expression profiling and interactive analyses. *Nucleic Acids Res* 2017; **45**: W98–W102.
  48. Huang J, Demmler R, Mohamed Abdou M, *et al.* Rapid qPCR-based quantitative immune cell phenotyping in mouse tissues. *J Invest Med* 2024; **72**: 47–56.
  49. Ostler N, Britzen-Laurent N, Liebl A, *et al.* Gamma interferon-induced guanylate binding protein 1 is a novel actin cytoskeleton remodeling factor. *Mol Cell Biol* 2014; **34**: 196–209.
  50. Schindelin J, Arganda-Carreras I, Frise E, *et al.* Fiji: an open-source platform for biological-image analysis. *Nat Methods* 2012; **9**: 676–682.
  51. Weinländer K, Naschberger E, Lehmann MH, *et al.* Guanylate binding protein-1 inhibits spreading and migration of endothelial cells through induction of integrin alpha4 expression. *FASEB J* 2008; **22**: 4168–4178.
- References [47–51] are cited only in the supplementary material.

## SUPPLEMENTARY MATERIAL ONLINE

### Supplementary materials and methods

**Figure S1.** Homology of peptide used for immunization to generate AMIGO2 antibodies in AMIGO1 and AMIGO3

**Figure S2.** AMIGO2 expression is increased in tumor stroma compared to normal colon tissue

**Figure S3.** AMIGO2 expression is higher in CAFs compared to NAFs in adjacent healthy and diseased tissues of CRC patients

**Figure S4.** AMIGO2 RNA expression is not related to CRC tumor grading

**Figure S5.** AMIGO2 expression is increased in liver metastasis compared to primary tumor

**Table S1.** Patient cohort for analysis of AMIGO2 expression in normal colon and CRC ( $n = 10$ )

**Table S2.** Prospectively collected patient cohort for analysis of AMIGO2 mRNA expression in RNA isolated from FFPE tissues ( $n = 338$ )

**Table S3.** Patients included for evaluation of AMIGO2 expression between UICC I and IV in colon cancer ( $n = 24$ )

**Table S4.** Patients included for evaluation of AMIGO2 expression primary tumor and liver metastasis in CRC ( $n = 7$ )

**Table S5.** Prospectively collected patient cohort for cancer-related survival analysis ( $n = 254$ )